Submitted to 2014 CSMANTECH Conference, Denver, Colorado (Student Paper)

Optimization of Selective Oxidation for 850 nm (IR) and 780 nm (Visible) Energy/Data Efficient Oxide-Confined Microcavity VCSELs

Michael Liu, Mong-Kai Wu, and Milton Feng

Department of Electrical and Computer Engineering · University of Illinois
Micro and Nanotechnology Laboratory · 208 N. Wright Street, Urbana, IL 61801
Phone: (217)244-3662, e-mail: meliu2@illinois.edu

INTRODUCTION

Vertical-cavity surface-emitting diode lasers (VCSELs) have gained broad interests in high speed and low noise optical transceivers. Recently, microcavity VCSELs have demonstrated higher bandwidth via Purcell enhancement while reducing power consumption and relative intensity noise (RIN) [1-3]. These advantages make microcavity VCSELs extremely useful especially in short-hub interconnect system. Recently, a microcavity VCSEL with an aperture dimension of 4.6μm at 850nm emission has passed 40Gb/s bit-error-rate test. A 2μm aperture microcavity VCSEL also has shown 40Gb/s open eye. The aperture size of a microcavity VCSEL is controlled by wet oxidation, and the oxidation rate and uniformity then become the keys to obtain consistent aperture size in a batch. In this paper, we address the oxidation uniformity issue and the possible solution.

DEVICE FABRICATION AND OXIDATION ISSUES

The epitaxial layers consist of 35 pairs of n-doped $Al_{0.12}Ga_{0.88}As/Al_{0.9}Ga_{0.1}As$ bottom DBR mirror, followed by undoped GaAs with three InGaAs quantum wells as the active region, and another 21 pairs of p-doped top DBR. Above the active region, there is an $Al_{0.98}Ga_{0.02}As$ layer serving as the oxidation layer, which can be oxidized as aluminum oxide for both electrical and optical confinement. P-type metal contact is first evaporated on the sample, and then SiN_x is deposited as an etching mask. With photoresist lithography and CF_4 dry etch, the SiN_x hard mask is patterned. The top DBR mirror is then etched by inductively coupled plasma (ICP) RIE through the active region. After the dry etching, the sample is transferred to an oxidation furnace at 425°C filled with N_2 and H_2O vapor mixed gas. Then, the bottom n-type contact is evaporated and alloyed. The sample is planarized with BCB. After via opening, 1 μm Ti/Au metal interconnect is evaporated, and the device is ready for testing. Figure 1 shows a SEM image of the finished device.

The main challenge of fabricating the microcavity VCSELs is to precisely control the aperture size. Figure 2 shows the measured spectra of 2 VCSELs on the same wafer. The variation in oxidation transfers to the laser spectrum profile. By estimating the mode spacing, the two devices are characterized to have oxide aperture diameters of 7 and 7.5 μm. When further reducing the oxide aperture diameter to below 3 μm, the inability to control the oxidation process will not only lead to device characteristics and performance variation on the wafer but also cause issues in yield. For microcavity VCSELs, a 0.5 μm difference may cause the threshold and mode spacing to vary more severely when compared to 7 and 7.5 μm oxide apertures.

The water vapor in our wet furnace is from a bubbler wrapped with heat tape and filled with DI water. We allow at least 3 hours for gas flow to stabilize in the furnace before the device oxidation process. The N_2 / H_2O mixing gas will escape from the furnace when opening the cap to load the sample. The sample loading time is then becoming a critical issue for having uniform oxidation in a batch. Typically, the sample loading should not be more than 20 seconds. After the wet oxidation, the sample will be moved into a dry N_2 furnace set at 410°C to drive out the moisture in the oxide layer. Figure 3 shows the SEM cross-section of a DBR mesa under wet oxidation for 7 minutes. It shows that even on a single mesa, the oxidation rate on different sides can vary. This issue is identified as unstable gas flow in the wet oxidation furnace due to excessive loading time. The longer the loading time is, the more incontrollable the oxidation process becomes. Figure 4 shows the threshold current of the devices for 2 VCSEL lot fabricated with the same process flow but different wet oxidation loading time. In the 780nm VCSEL process, the loading time for the oxidation was controlled to around 20 seconds; however, in the 850nm VCSEL process, the loading time was over 30 seconds. The 850nm VCSELs show variation from 0.66 to 0.98 mA for the current threshold with a standard deviation of 0.0887mA. On the other hand, for most of the 780nm VCSELs, their threshold current is in the range of 0.65-0.75 mA with a standard deviation of 0.032mA. The threshold current is proportional to the volume of the active region in a VCSEL, and the lateral dimensions of the active region are controlled by the oxide aperture. From the data in Figure 4, oxidation process control plays an important role in the uniformity of device characteristics.

DEVICE CHARACTERISTICS AND RESULTS

Figure 5 shows the emission spectrum of a 2 μm diameter microcavity VCSEL at 0.28mA. It shows mode spacing of 3nm and a side mode suppression ratio (SMSR) of 36.3dB, which is considered as single mode operation. Figure 6 shows the optical frequency response of the microcavity laser under I/I_{TH} = 3, 6, and 10, respectively. The optical bandwidth increases from 13.9 GHz to 22.5 GHz. The optical response does not show large resonant bump, which indicates the recombination rate is enhanced by Purcell enhancement. The Agilent 81250 43.2 Gb/s ParBERT signal generator is used to generate the 20 and 40 Gb/s NRZ $2^{15} - 1$ bit length pseudorandom binary series pattern with 0.5 V_{pp} ac voltage swing for eye diagram measurement. Figure 7 shows the eye diagram at 20 Gb/s and 40 Gb/s data rates of the 2-μm aperture VCSEL under 1.5 mA (I/I_{TH} = 10) at 15°C. The microcavity laser shows an open eye at 20 and 40 Gb/s data rates. The data-energy efficiency of the microcavity VCSEL is determined as 11.29 Gb/s/mW.

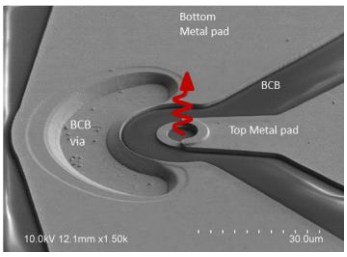

Figure 1. the SEM image of microcavity VCSEL

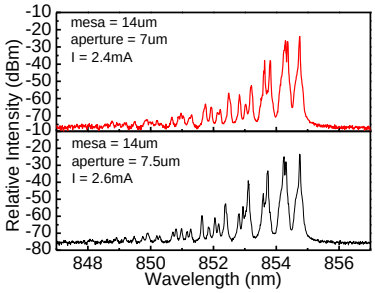

Figure 2. The emission spectra of two 7 μm VCSEL on the same

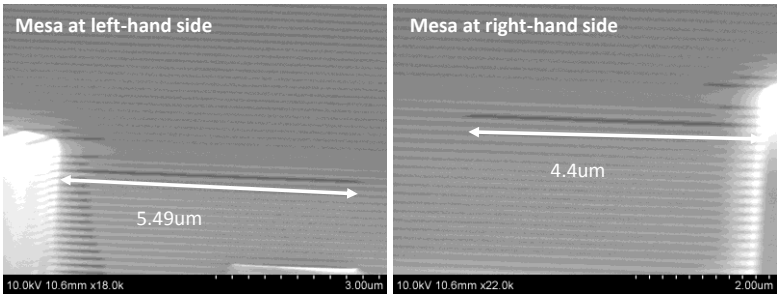

Figure 3. The cross section of a DBR mesa after oxidation in the unstable finance for 7minutes

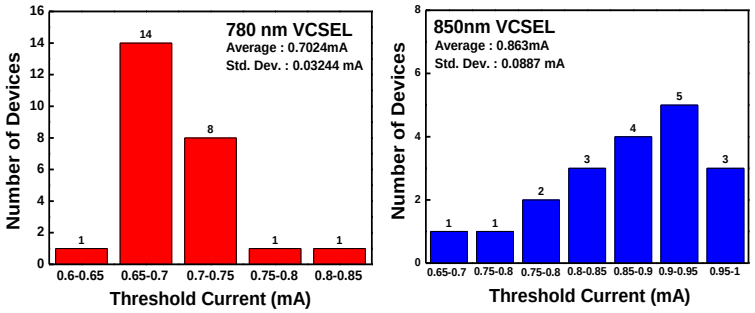

Figure 4. The threshold current distribution for 2 VCSEL

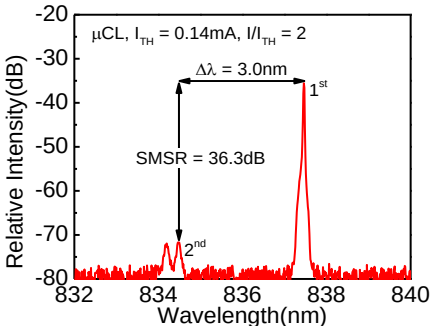

Figure 5. The spectra of the 2 μm microcavity

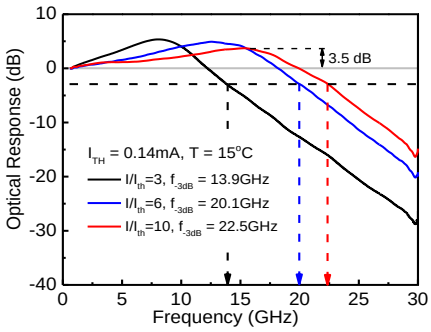

Figure 6. Frequency response of 2 μm microcavity laser

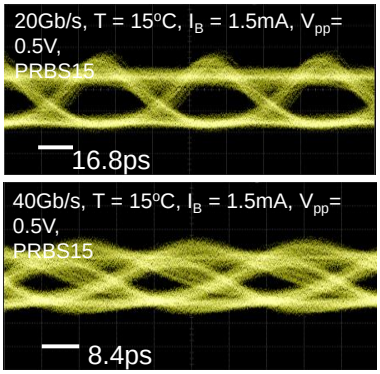

Figure 7. Eye diagrams at 20 Gb/s an 40 Gb/s data rates for 2 μm aperture microcavity laser

REFERENCES

[1] F. Tan, C.H. Wu, M. Feng, and N. Holonyak, Jr., "Energy Efficient Microcavity Lasers with 20 and 40Gb/s data transmission," Appl. Phys. Lett. 98, 191107 (2011)

[2] F. Tan, M.K. Wu, M. Liu, M .Feng, and N. Holonyak, Jr., "850 nm Oxide-Confined VCSEL with Ultralow Laser Relative Intensity Noise and 40Gb/s Error Free Data Transmission", To be published on IEEE Photon. Technol. Lett. (2013) (doi: 10.1109/LPT.2013.2280726)

[3] F. Tan, M.K. Wu, M. Liu, M. Feng, and N. Holonyak, Jr., "Relative Intensity Noise in High Speed Microcavity Laser", Appl. Phys. Lett. 103, 141116 (2013)